Molecular Therapy
Methods & Clinical Development
Original Article

Preclinical safety assessment of MV-s-NAP, a novel oncolytic measles virus strain armed with an *H. pylori* immunostimulatory bacterial transgene

Kimberly B. Viker,[1,4] Michael B. Steele,[1,4] Ianko D. Iankov,[1] Susanna C. Concilio,[1] Arun Ammayappan,[1] Brad Bolon,[2] Nathan J. Jenks,[1] Matthew P. Goetz,[3] Eleni Panagioti,[1,5] Mark J. Federspiel,[1] Minetta C. Liu,[3] Kah Whye Peng,[1] and Evanthia Galanis[3]

[1]Department of Molecular Medicine, Mayo Clinic, Rochester, MN 55905, USA; [2]GEMpath, Inc., Longmont, CO 80501, USA; [3]Department of Oncology, Mayo Clinic, Rochester, MN 55905, USA

Despite recent therapeutic advances, metastatic breast cancer (MBC) remains incurable. Engineered measles virus (MV) constructs based on the attenuated MV Edmonston vaccine platform have demonstrated significant oncolytic activity against solid tumors. The *Helicobacter pylori* neutrophil-activating protein (NAP) is responsible for the robust inflammatory reaction in gastroduodenal mucosa during bacterial infection. NAP attracts and activates immune cells at the site of infection, inducing expression of pro-inflammatory mediators. We engineered an MV strain to express the secretory form of NAP (MV-s-NAP) and showed that it exhibits anti-tumor and immunostimulatory activity in human breast cancer xenograft models. In this study, we utilized a measles-infection-permissive mouse model (transgenic IFNAR KO-CD46Ge) to evaluate the biodistribution and safety of MV-s-NAP. The primary objective was to identify potential toxic side effects and confirm the safety of the proposed clinical doses of MV-s-NAP prior to a phase I clinical trial of intratumoral administration of MV-s-NAP in patients with MBC. Both subcutaneous delivery (corresponding to the clinical trial intratumoral administration route) and intravenous (worst case scenario) delivery of MV-s-NAP were well tolerated: no significant clinical, laboratory or histologic toxicity was observed. This outcome supports the safety of MV-s-NAP for oncolytic virotherapy of MBC. The first-in-human clinical trial of MV-s-NAP in patients with MBC (ClinicalTrials.gov: NCT04521764) was subsequently activated.

INTRODUCTION

Breast cancer is the most common malignancy in women and also the second leading cause of female cancer mortality in the United States.[1] Despite the availability of a growing therapeutic arsenal of biologic and chemical agents including endocrine therapy, chemotherapy, targeted agents, and immunotherapy, metastatic breast cancer (MBC) remains incurable.[2,3] The field of immunotherapy is expanding quickly throughout oncology, but to date, breast cancer studies focused on vaccines and immune checkpoint antagonists have achieved only modest success, with the only notable exception being the recent approval of an anti-PD1 antibody for a subgroup of triple negative breast cancer patients.[4–6]

To date, only one oncolytic virus platform, a herpes simplex virus 1 (HSV-1) construct engineered to express granulocyte-macrophage colony-stimulating factor (GM-CSF) (talimogene laherparepvec [T-VEC]), is commercially available for treatment of solid tumors in the United States and Europe.[7–9] Intratumoral injection of T-VEC (Imlygic) has resulted in single-agent efficacy in patients with recurrent melanoma with a favorable adverse-effect profile.[9–11] Case reports of patients with breast cancer included in phase I trials of oncolytic virotherapy suggest the potential of clinical benefit from this approach.[12–16] We hypothesized that rational development of oncolytic platforms with activity against breast cancer, such as measles virus (MV), can create novel, potent therapies against this disease. MV is an enveloped paramyxovirus with a negative-sense single-stranded RNA genome. Wild-type MV enters cells by binding of its hemagglutinin (HA) attachment protein to one of two cellular receptors: Nectin-4 or signaling lymphocyte activation molecule (SLAM). The live, attenuated, non-pathogenic MV Edmonston vaccine strain (MV-Edm) enters cells using any of three known receptors, CD46, SLAM, or Nectin-4. Both CD46 and Nectin-4 expression is upregulated on breast cancer cells.[17]

MV-Edm infection of cancer cells leads to extensive intercellular fusion (syncytia) followed by cell death.[18] MV-Edm causes minimal or no cytopathic effect in non-transformed cells.[19] Engineered MV constructs based on the attenuated MV-Edm strain have demonstrated oncolytic properties and significant anti-tumor activity

Received 10 January 2022; accepted 20 July 2022;
https://doi.org/10.1016/j.omtm.2022.07.014.

[4]These authors contributed equally

[5]Present address: Brigham and Women's Hospital, Department of Neurosurgery, Boston, MA 02115

Correspondence: Evanthia Galanis, MD, Mayo Clinic, 200 First Street SW, Rochester, MN 55905, USA.
E-mail: galanis.evanthia@mayo.edu

Table 1. Toxicology study design and treatment groups assessed in this study

	Group name	Buffer s.c.	MV-s-NAP (1×10^6 s.c.)	MV-s-NAP (1×10^7 s.c.)	Buffer IV	MV-s-NAP (1×10^6 i.v.)	MV-s-NAP (1×10^7 i.v.)
	Treatment	buffer	MV-s-NAP	MV-s-NAP	buffer	MV-s-NAP	MV-s-NAP
	Dose ($TCID_{50}$)	NA	1×10^6	1×10^7	NA	1×10^6	1×10^7
	Dose route	s.c.	s.c.	s.c.	i.v.	i.v.	i.v.
Single	Number of doses	1	1	1	1	1	1
	Number of mice	8	8	8	8	8	8
	Harvest day	11	11	11	12	12	12
Multiple	Number of doses	3	3	3	3	3	3
	Number of mice	8	8	8	8	8	8
	Harvest day	56	56	56	54	54	54

Single (treatment) refers to mice that received one dose of MV-s-NAP and were euthanized at day 11 (s.c. group) or 12 (i.v. group). Multiple (treatments) refers to mice that received three doses of MV-s-NAP and were euthanized on day 56 (s.c. group) or 54 (i.v. group). MV-s-NAP doses are presented as amount (1×10^6 [1×10^6] or 1×10^7 [1×10^7]) relative to the 50% tissue culture infectious dose ($TCID_{50}$). s.c., subcutaneous; i.v., intravenous; NA, not applicable.

against multiple solid tumors *in vitro* and *in vivo*.[20] In addition, MV-Edm has an outstanding safety record with millions of doses administered annually for human immunization against measles.[21] Few severe adverse events and no cases of subacute sclerosing panencephalitis (SSPE), a rare fatal complication of wild-type MV infection, have been reported as a result of vaccination with MV-Edm.[22–24]

Bacterial cell-wall components and released intracellular factors are potent immunostimulators that have been evaluated as adjuvant components in formulated vaccines.[25] *Helicobacter pylori* neutrophil-activating protein (NAP) is a key trigger of the robust inflammatory reaction observed in the gastroduodenal mucosa following *H. pylori* infection. NAP attracts innate immune cells such as neutrophils and macrophages to the site of infection and promotes production of reactive oxygen species (ROS) and expression of many pro-inflammatory mediators.[26,27] As a potent Toll-like receptor 2 (TLR2) agonist, NAP stimulates the release of T helper type 1 (Th1) cytokines, including interleukin-12 (IL-12) and IL-23, and chemokines, thereby inducing Th1-type polarization of the immune response.[28,29] Our laboratory has cloned the secretory form of NAP (s-NAP) into MV-Edm, and in proof-of-principle studies, we have demonstrated the anti-tumor activity of MV constructs and MV-s-NAP against both subcutaneous models and a mouse pleural effusion model of MBC.[30–33] NAP expression by infected tumor cells in these models resulted in the induction of a strong Th1 immune response with increased levels of pro-inflammatory cytokines such as IL-12/-23, IL-6, and tumor necrosis factor alpha (TNF-α) in pleural fluid and IL-6 in serum. No toxicity was observed in these models.[30]

Prior to clinical translation of a first-in-human trial of MV-s-NAP in MBC (ClinicalTrials.gov: NCT04521764; principal investigator [PI]: M.C.L.), we performed preclinical toxicity studies to examine the biodistribution and evaluate the safety of the MV-s-NAP platform in measles replication-susceptible IFNAR KO-CD46Ge mice. These animals have a targeted mutation inactivating the interferon-α/β receptor (IFNAR) and express the human CD46 gene in a distribution that mimics the distribution in humans.[34] Although murine cells are not infectable by MV, this transgenic model allows MV infection and propagation and has been accepted by the US Food and Drug Administration (FDA) as a small-animal toxicology model in support of human trials for oncolytic MV strains. The primary objective of this study was to define the highest dose of injected MV-s-NAP that will not result in toxicity, when the virus is administered locally within the subcutaneous tissues, which mimics as closely as possible the direct intratumoral route of administration proposed in the clinical trial. Due to intact T and B cell immunity, IFNAR KO-CD46Ge mice do not allow the growth of human tumor xenografts; as such, toxicology testing of oncolytic MV strains in MV-replication-permissive tumor-bearing mice is not possible. Per FDA's recommendation, intravenous administration was added to this toxicity study in order to address a "worst-case" scenario in which the virus would gain access to the bloodstream and spread systemically.

Here, we report that both subcutaneous (s.c.) and intravenous (i.v.) delivery of MV-s-NAP, an oncolytic MV construct expressing the immunostimulatory s-NAP transgene, were well tolerated and resulted in minimal histopathologic abnormalities *in vivo*. This outcome supports the *in vivo* safety of this agent and led to activation of the first-in-human trial for clinical investigation of the MV-s-NAP platform in patients with MBC.

RESULTS

Study design

A detailed description of the study design is included in the materials and methods and in Table 1. In summary, mice received either a single virus treatment or three virus treatments over a 28-day period. For each treatment schedule cohort, 8 mice per group received either buffer (control) or MV-s-NAP at either 1×10^6 median tissue culture infectious dose ($TCID_{50}$) or 1×10^7 $TCID_{50}$ by either the s.c. or i.v. route for a total of 96 animals. Virus-treated mice that received a single dose were euthanized on day 11 or 12. Mice that received multiple (3) doses were euthanized on day 54 or 56. The 1×10^7 $TCID_{50}$ dose in this toxicology study is equivalent to 350× the initial proposed dose in the human trial. The

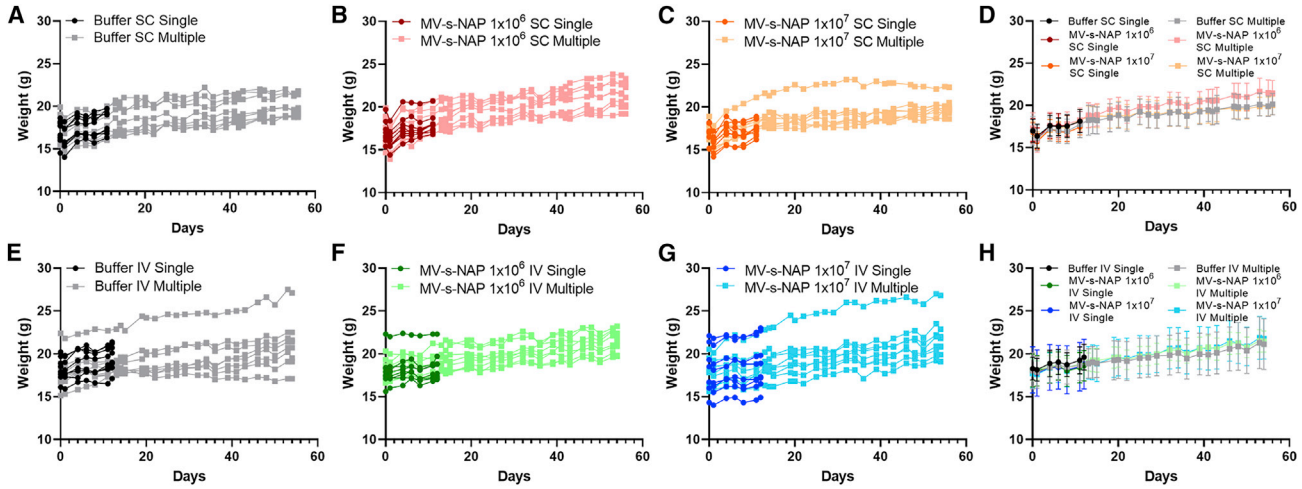

Figure 1. Treatment with MV-s-NAP did not affect body weight

Single refers to mice that received one dose of MV-s-NAP and were terminated on day 11 (s.c. group) or day 12 (i.v. group). Multiple refers to mice that received three doses of MV-s-NAP and were terminated on day 56 (s.c. group) or day 54 (i.v. group). Each line represents a single animal in that group. (A) Animal weights in the s.c. single or multiple injection groups that received buffer. (B) Animal weights in the s.c. single or multiple injection groups that received $1x10^6$ MV-s-NAP. (C) Animal weights in the s.c. single or multiple injection groups that received $1x10^7$ MV-s-NAP. (D) Mean and standard deviation of animal weights in the s.c. injected groups. (E) Animal weights in the i.v. single or multiple injection groups that received buffer. (F) Animal weights in the i.v. single or multiple injection groups that received $1x10^6$ MV-s-NAP. (G) Animal weights in the i.v. single or multiple injection groups that received $1x10^7$ MV-s-NAP. (H) Mean and standard deviation of animal weights the i.v. injected groups.

2-week repeat administration schedule in the toxicology study versus 3 weeks in the human trial was chosen in order to increase dose intensity and simulate a worst-case scenario.

Body weight and survival

All groups were observed for clinical signs of toxicity, and body weight was measured at least 5 times per week for the duration of the study. Animal weights remained stable throughout the study (Figure 1). All mice were observed to be clinically normal throughout the experiment, and all animals survived to the end of the study. These results indicate that both a single dose and intermittently repeated treatments with MV-s-NAP do not induce clinically adverse health effects.

Hematologic and biochemical monitoring

Hematologic analysis of non-clotted whole blood consisted of an automated complete blood count (CBC) with differential cell count were obtained at the time of euthanasia. Blood cell parameters, including the number of white blood cells (WBCs), lymphocytes (LYMs), and platelets (PLTs) that would be expected to be impacted by an active viral infection, were not significantly different compared with control groups (Figure 2). These results indicate that MV-s-NAP treatment does not negatively impact hematologic function.

Clinical chemistry analysis of plasma samples was obtained at the time of euthanasia to evaluate potential liver and kidney toxicity, electrolytes, calcium, and glucose. Plasma activities of alkaline phosphatase (ALP) and alanine and aspartate aminotransferases (ALT and AST, respectively) were within normal limits for the animals that received MV-s-NAP, with a few exceptions: one mouse (of 8) in the single-dose s.c. group at day 11 showed elevated ALT, and two mice (of 8) in the multiple-dose i.v. group at day 54 exhibited higher ALT and AST activities. These altered values in individual mice were associated with hemolysis during collection of blood, which can interfere with liver enzyme analysis. All other serum chemical parameters were normal. These results indicate that MV-s-NAP treatment does not significantly impact liver or kidney function or other key metabolic processes (Figure 2).

Cytokine assays

A multiplex assay (IL-1β, IL-2, IL-4, IL-5, IL-6, IL-12, IL-13, IL-18, IFN-γ, GM-CSF, and TNF-α) was performed to determine the possible effect of single or multiple doses of MV-s-NAP on immunostimulatory cytokine expression. This analysis was performed to ensure that the immunostimulatory potential of NAP did not lead to an adverse systemic pro-inflammatory cytokine response (i.e., a "cytokine storm"). A systemic pro-inflammatory response was not observed in any of the groups treated with MV-s-NAP. In addition, the majority of samples for control and treated animals tested below the limit of detection (LOD) for the assay. Detectable cytokine expression was limited to IL-18 (following i.v. and s.c. administration) and TNF-α (after i.v. delivery only). However, plasma cytokine expression levels of both IL-18 and TNF-α were comparable between control and treated mice (Figure 3).

Biodistribution analysis

Gene expression of MV-nucleocapsid protein RNA (MV-N), by quantitative real-time reverse transcription PCR of total RNA,

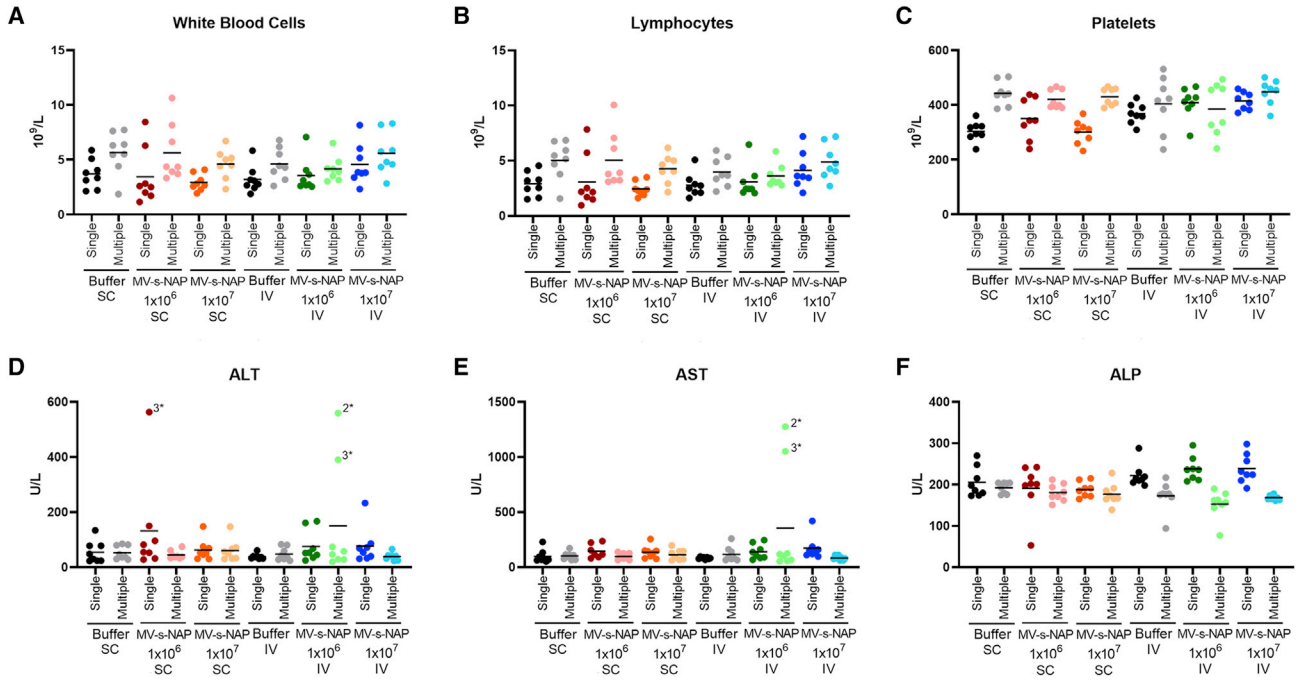

Figure 2. Treatment with MV-s-NAP does not impact hematologic parameters or liver function

(A–F) Evaluation of laboratory parameters at the time of scheduled euthanasia included (A) white blood cells, (B) lymphocytes, (C) platelets, (D) alanine aminotransferase (ALT), (E) aspartate aminotransferase (AST), and (F) alkaline phosphatase (ALP). Single (treatment) refers to mice that received one dose of MV-s-NAP and were necropsied on day 11 (s.c. group) or 12 (i.v. group). Multiple (treatments) refers to mice that received three doses of MV-s-NAP and were necropsied at day 56 (s.c. group) or 54 (i.v. group). s.c., subcutaneous; i.v., intravenous. Bars indicate group means. Due to the number of potential comparisons, statistical significance is only indicated if $p < 0.05$. 2*/3* next to individual values indicates hemolysis of the blood sample, which can artificially increase the detected activities of ALT, AST, and ALP.

was performed to assess viral distribution following s.c. or i.v. administration (Figure 4). As expected, expression following s.c. (local) injection was primarily found near the site of administration. In contrast, viral genomes were detected in several organs following i.v. (systemic) injection. S.c. administration of the MV-s-NAP, which was conducted to simulate the proposed intratumoral route of administration in clinical trial patients, resulted in low viral-genome copy numbers (close to the assay detection limits) on day 11 in the inguinal lymph nodes (i.e., the regional lymphoid organ closest to the injection site) of 2–3 (of 8) animals that received a single injection. No animals in the high-dose s.c. group had detectable MV RNA on day 56 after three MV-s-NAP SC injections (the last of which occurred on day 28).

Administration of the MV-s-NAP via the i.v. route resulted in the detection of viral genomes in most organs on day 11 (after one injection) in both the low- and high-dose groups. Among animals that received three virus injections, the low-dose mice had detectable MV-s-NAP genomes in brain (2/8 animals), lung (2/8 animals), liver (2/8 animals), spleen (8/8 animals), kidney, heart, spinal cord, ovary, bone marrow, small intestine, and large intestine (1/8 animals) on day 54. There were no detectable viral copy numbers in the inguinal lymph nodes or the stomach. Following three virus injections in the high-dose i.v. group, viral genomes were detected in multiple organs but not in the gastrointestinal (GI) tract, i.e., stomach, small intestine, or large intestine.

Histopathologic findings

Two main changes occurred following MV-s-NAP administration: limited acute hemorrhage in the lung and leukocyte infiltration or inflammation in skin at the s.c. injection site. Hemorrhage in the lung occurred as one or a few small regions of erythrocyte accumulation in randomly dispersed alveoli (Figure 5A). This change was always of minimal (i.e., one or two foci comprised of 2–4 affected alveoli per lobe) or occasionally mild (i.e., three to five foci comprised of 5–10 affected alveoli per lobe) severity. The involved alveoli typically contained, but were not occluded by blood, indicating that neither airway patency nor lung function was compromised; moreover, affected alveoli exhibited no evidence of cell disruption impacting either capillary endothelium or pneumocytes. Following s.c. injection, this finding was observed at minimal severity at day 11 in 1–2 mice in both dose groups. No hemorrhage was observed on day 56. Following i.v. injection, this change was seen on day 11 in 1 (of 8) animal which received the high viral dose and on day 54 in 5 (of 8) low-dose mice and 1 (of 8) high-dose animal. A possible explanation for this finding in only a few treated animals, independent of dose level and route of administration, is the use of carbon dioxide in euthanasia (which commonly produces focal agonal alveolar hemorrhage in rodents as

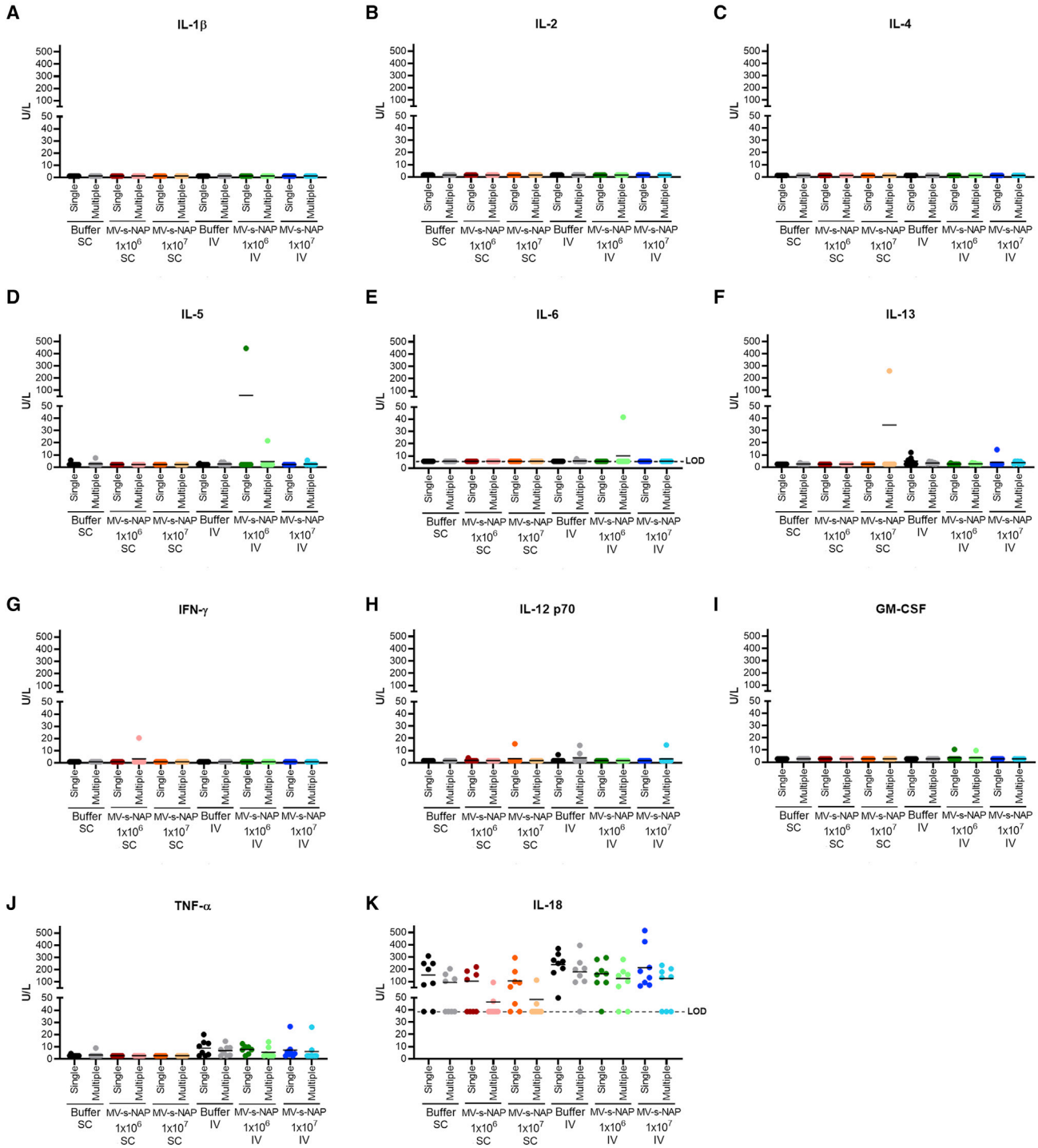

Figure 3. Treatment with MV-s-NAP does not increase circulating levels of pro-inflammatory cytokines in plasma

Single (treatment) refers to mice that received one dose of MV-s-NAP and were euthanized on day 11 (s.c. group) or day 12 (i.v. group). Multiple (treatments) refers to mice that received three doses of MV-s-NAP and were euthanized on day 56 (s.c. group) or day 54 (i.v. group). Panels A-K depict circulating levels of proinflammatory cytokines in s.c. and i.v. treated mouse groups for both the single and multiple administration schedule. Each panel represents the results for a single cytokine as follows: (A) IL-1β. (B) IL-2. (C) IL-4. (D) IL-5. (E) IL-6. (F) IL-13. (G) IFN-γ. (H) IL-12 p70. (I) GM-CSF. (J) TNF-α. (K) IL-18; s.c., subcutaneous; i.v., intravenous; IFN-γ, interferon gamma; GM-CSF, granulocyte-macrophage colony-stimulating factor; TNF-α, tumor necrosis factor alpha; LOD, limit of detection. Bars indicate group mean. Due to the number of potential comparisons, statistical significance is only indicated if $p < 0.05$.

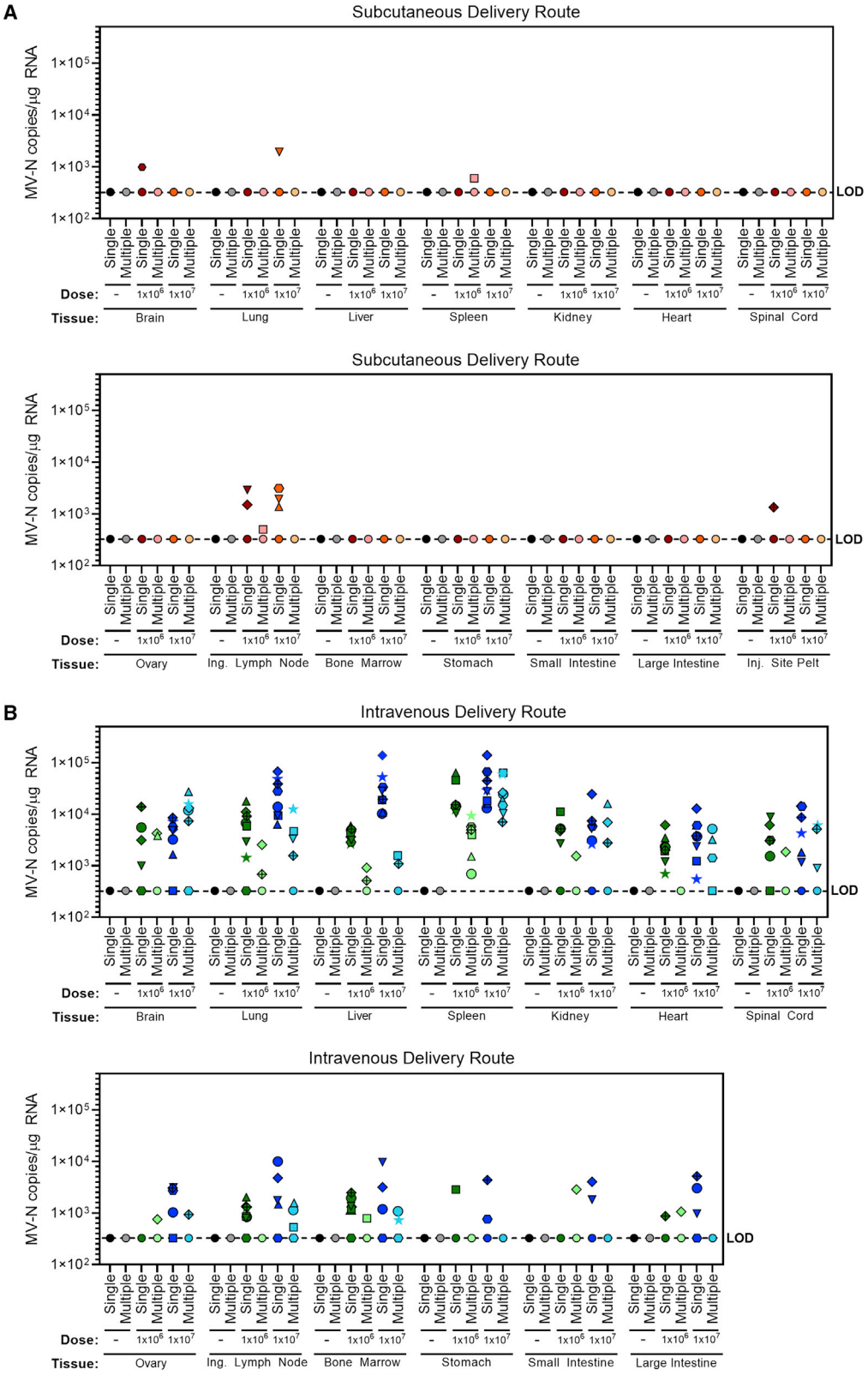

(legend on next page)

an incidental artifact).[35] Still, these changes were limited, transient, self-resolving, and they were not associated with clinical signs of toxicity at any time point. At the MV-s-NAP s.c. injection site, mononuclear cell infiltration (i.e., groups of leukocytes, usually lymphocytes and occasional macrophages, without any damage to the resident tissue) and inflammation (i.e., groups of leukocytes, typically a mixture of mononuclear cells and a few neutrophils resulting in limited damage to the injected tissue), were localized to the deep dermis and subcutis in 1 or 2 animals per 8 animal group (Figure 5B). Granulation tissue (i.e., dense, fibrous connective tissue new blood vessels) without infiltration or inflammation was noted rarely in both treated and control mice. All these changes were focal and of minimal degree and thus were interpreted to be not significant.

Antibody assays

Anti-MV and anti-NAP assays were performed to determine antibody responses to MV-s-NAP administration. Antibody responses occurred following administration by either route. The responses were more consistent in incidence and extent following i.v. injection and were more commonly mounted against the MV antigens (Figure 6). Following i.v. injection, administration of MV-s-NAP resulted in a strong early response against the MV antigens, reaching titers of 1:12,800 in all mice of both dose groups following a single injection by day 12. High anti-MV titers of 1:12,800–51,200 were maintained on day 54 following three i.v. injections in all animals of both dose groups. Anti-NAP antibodies were observed on day 11 (following one injection) in the high-dose group only and in some animals for both dose levels at day 54 (following three injections). In general, the anti-NAP response was characterized by substantially lower titers than detected for the anti-MV response. For s.c. injection, administration of MV-s-NAP led to antibody responses in only one or two mice in both dose groups on day 11, and these were limited primarily to antibodies against MV. In contrast, repeated test-article injection generated strong anti-MV responses above 1:12,800 (1:51,200 in 3 animals) in all mice treated with the high dose and in 6 (of 8) mice given the lower dose. One mouse (of 8) treated with a single low dose of MV-s-NAP exhibited a robust anti-NAP response (1:20,480) (Figure 6).

DISCUSSION

MV-induced oncolytic cell death has immunostimulatory properties.[36–38] In order to maximize this immunostimulatory potential, we sought to engineer the virus with a transgene that can cause broad and robust immune system activation. *H. pylori* NAP is a potent immunomodulator of bacterial origin. NAP attracts immune cells and promotes expression of mediators of inflammation. As a potent TLR2 agonist, NAP stimulates the Th1 polarization of the immune response. Our team engineered the MV-Edm backbone to express s-NAP. Intrapleural administration of MV-s-NAP doubled the survival time of treated animals in an aggressive model of MBC with lung metastases.[26] Secretory NAP was expressed at high levels by the infected tumor cells, and we detected increased levels of the pro-inflammatory cytokines TNF-α, IL-6, and IL-12/-23 in the pleural effusion.[30] Combination of MV-s-NAP with immune checkpoint inhibitors demonstrated synergistic activity in syngeneic mouse models.[38] These data support that the addition of a transgene encoding the NAP immunomodulator could further enhance the efficacy of MV strains to create novel immunovirotherapy approaches for the treatment of MBC.

These strong preclinical data justified clinical translation in a first-in-human trial. The primary goals of this phase I study in patients with MBC are to determine the maximum tolerated dose, safety, and toxicity of single or repeated intratumoral administration of MV-s-NAP. In support of this investigational new drug (IND), a preclinical toxicity study (as described in this article) was designed with FDA's input. Our work presented here represents the first formal assessment of the toxicity and biodistribution of a MV derivative expressing the TLR2 receptor agonist NAP; this is a novel immunostimulatory approach never previously tested in the context of an oncolytic platform.

Our toxicity study was conducted in non-tumor-bearing female IFNAR KO-CD46Ge, a transgenic model that is permissive to MV replication. We investigated the effects of MV-s-NAP both administered via the intended local (s.c.) route but also administered i.v. to address the scenario of inadvertent systemic administration. Both single-dose (day 0) and multiple-dose administration schedules (days 0, 14, and 28) were tested. MV strains cannot infect or replicate in murine cells, as mice do not express MV receptors; the IFNAR KO-CD46Ge mice lack expression of the IFN- α/β receptor, allowing for viral replication in murine cells, and express human CD46 (a ubiquitous MV receptor) in a biodistribution similar to humans, thus allowing human-mimetic MV replication in mice.[34] This measles-replication-permissive model has been accepted by the FDA as an appropriate system for assessing the toxicity of MV constructs prior to translation to humans for indications such as ovarian cancer and primary brain tumors.[39,40] In our current study, all MV-s-NAP-treated IFNAR KO-CD46Ge mice survived to the end of study and thrived, as indicated by consistent growth after an initial minimal and transient weight loss. In addition, all treated mice exhibited the expected appearance and behaviors throughout the study at all dose levels and schedules.

The highest viral dose administered to the mice in this study was 1×10^7 $TCID_{50}$. Administration of this dose to a 20-g mouse is

Figure 4. Quantification of MV-s-NAP genomes recovered from tissues as detected by quantitative real-time reverse transcription PCR

(A) MV-s-NAP genome detection in mice treated via the s.c. route. (B) MV-s-NAP genome detection in mice treated via the i.v. route. Single refers to mice that received one dose of MV-s-NAP and were euthanized on day 11 (s.c. group) or day 12 (i.v. group). Multiple refers to mice that received three doses of MV-s-NAP and were euthanized on day 56 (s.c. group) or day 54 (i.v. group). Each point represents a single mouse with detectable genome copies. LOD, limit of detection: 1,000 copies per μg RNA. Tissue name abbreviations: Ing., inguinal; Inj., injection.

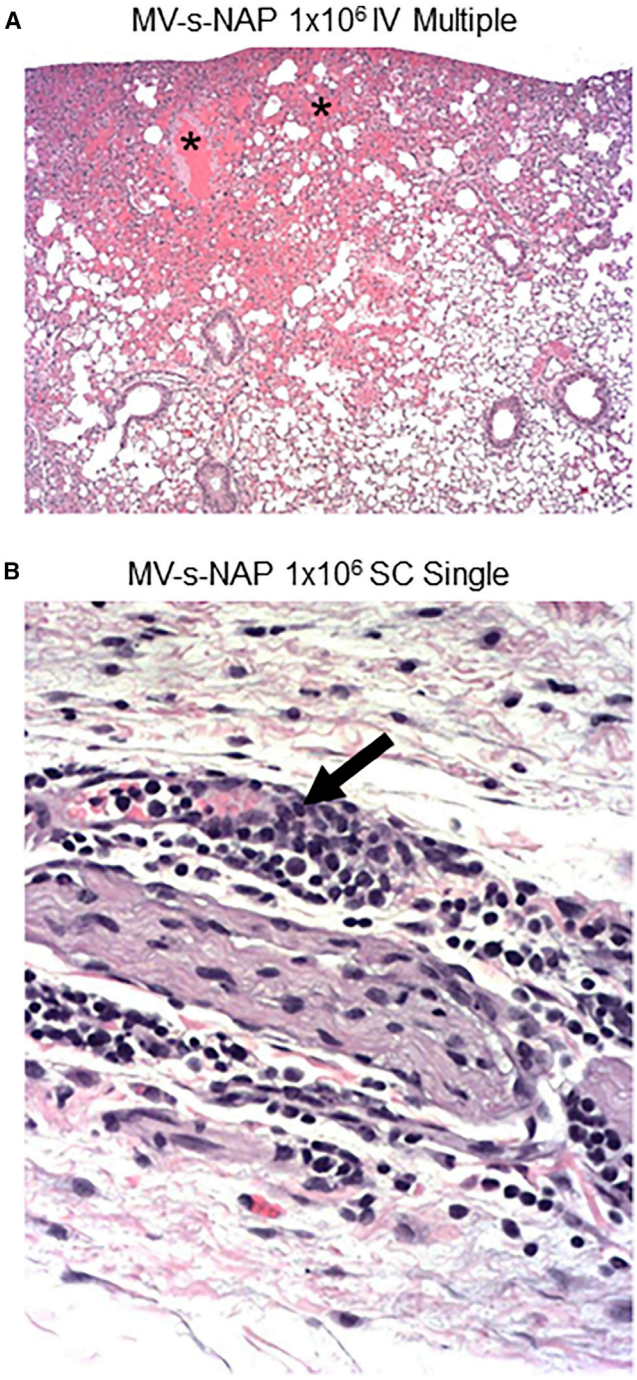

Figure 5. Minor histopathological findings in MV-s-NAP treated mice

(A) H&E stain of lung tissue. Minimal hemorrhage observed in lungs of a mouse treated with multiple (3) 1×10^6 TCID50 doses of MV-s-NAP via the i.v. route. Asterisks indicate small foci of acute intraalveolar hemorrhage (indicated by intact red blood cells) surrounding small blood vessels. Original objective magnification 20×. (B) H&E stain of injection site skin. Limited possible MV-s-NAP-related effects following s.c. administration in mouse treated with a single 1×10^6 dose MV-s-NAP via the s.c. route. Arrow indicates small foci of mononuclear cell infiltration (i.e., leukocyte accumulation with no damage to the involved tissue) and rarely inflammation (accumulation with damage to the local tissue). Original objective magnification 4×.

equivalent to 350× the initial dose proposed in the human trial (1×10^7 $TCID_{50}$ in a 70 kg adult patient) and 3.5× the highest proposed dose (1×10^8 $TCID_{50}$). The safety profile observed in mice at such a high MV-s-NAP dose suggests a large window for dose escalation in human patients.

Hepatoxicity due to uptake and sequestration of oncolytic viruses by hepatocytes is a common concern.[41–43] Our viral biodistribution studies and pathology evaluations indicated that administration of MV-s-NAP was safe when injected once or several times at very high doses into IFNAR KO-CD46Ge mice. By quantitative real-time reverse transcription PCR, liver tissue had high levels of MV-N RNA on day 12 after a single i.v. injection, but the amount of MV-N RNA decreased below the LOD by day 56 (i.e., approximately 4 weeks after the third i.v. injection on day 28). The expression levels of MV-N RNA were dose dependent. In contrast, RNA copies were not detected in the liver after one or multiple s.c. injections, mimicking the route being tested in the clinical trial. Of note, liver-function tests (including the liver enzymes ALP, ALT, and AST) were within normal limits after i.v. or s.c. injection of MV-s-NAP, further supporting its safety and lack of a negative impact on liver function (Figure 2).

Circulating levels for ten key pro-inflammatory cytokines were either not detectable in serum (IL-1β, IL-2, IL-4, IL-5, IL-6, IL-12, IL-13, IFN-γ, GM-CSF) or were limited to levels that were comparable to those measured in control animals (IL-18 following i.v. and s.c. administration, TNF-α after i.v. delivery only) (Figure 3). Histopathological findings following the course of MV-s-NAP treatment were minimal and were confined to a very low incidence of limited acute hemorrhage in the lung following i.v. or s.c. delivery and minimal mononuclear cell infiltration or occasionally inflammation localized at the s.c. injection site. The lung hemorrhage was assessed by the veterinary pathologist to likely be an artifact related to the euthanasia method.[35] This interpretation is supported by the presence of this finding in only a few treated mice and the lack of association with dose and route of administration. The leukocyte infiltration and inflammation at the injection site was deemed to be minor and unlikely to result in clinical signs or progressive inflammation. Overall, these structural changes at the injection site and in the lung would not be expected to impact the function of the affected tissues and, over time, would have been repaired without leaving any residual changes of consequence. Other organs, including the liver, were histologically normal in appearance following MV-s-NAP treatment. The overall interpretation of these findings is that one or repeated injections of MV-s-NAP either locally (s.c., as a surrogate for direct intratumoral delivery) or systemically (i.v.) produces no adverse effects. Therefore, this oncolytic viral therapeutic agent is expected to be safe and well tolerated when administered into tumors of patients with MBC.

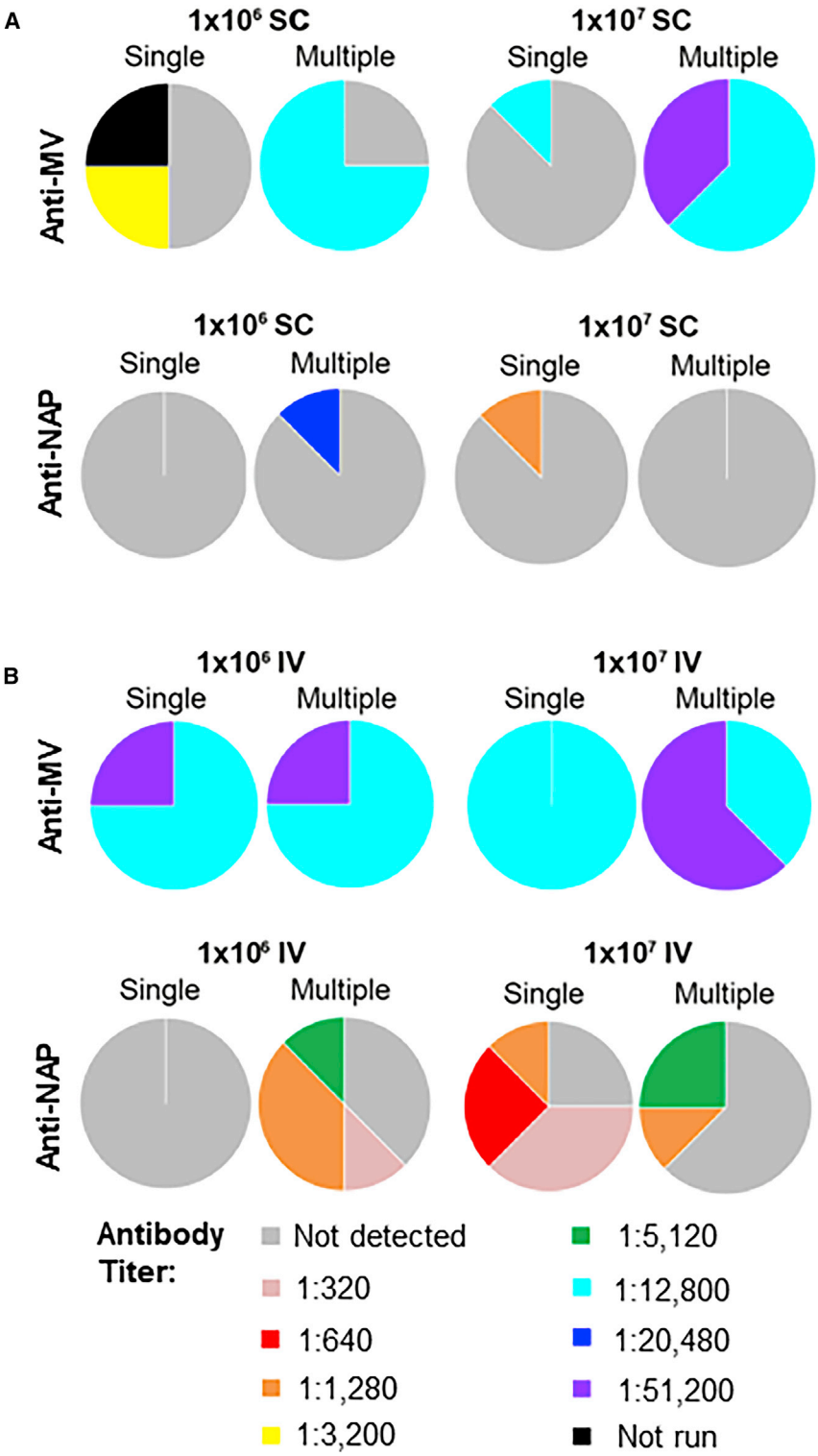

Figure 6. Antibody responses to measles virus and NAP protein

Antibody production against MV or NAP protein was assessed via ELISA. Each pie represents all eight animals in each group. (A) Antibody titers in mice treated via the s.c. route. (B) Antibody titers in mice treated via the i.v. route. Anti-MV antibodies were not assessed in two mice in the single 1×10^6 s.c. dose group due to insufficient serum volume.

These results mirror previous studies in IFNAR KO-CD46Ge mice infected via intranasal, intraperitoneal, i.v., intracerebral, intraventricular, or intrahepatic routes with different MV-Edm derivatives in that no significant changes in hematology, coagulation, blood chemistry, hepatic and kidney function, or immunosuppression were detected and any histopathologic changes were minimal.[34,39,40,44–47] Toxicology studies in squirrel monkeys and rhesus macaques with MV-Edm constructs inoculated intratracheally, intranasally, intracerebrally, intraventricularly, or intrahepatically similarly resulted in lack of clinical or histologic toxicity.[46–49] Our study adds to the ever-growing body of data indicating that MV-Edm derivatives are safe and well tolerated.

As expected, our results confirmed that biodistribution of MV-s-NAP depends on the route of administration (Figure 4). Following s.c. administration, viral RNA was below detectable levels by quantitative real-time reverse transcription PCR except for the draining lymph node and, rarely, other well-vascularized organs at very low levels. Therefore, s.c. injection, which closely mimics intratumoral injection in patients, results primarily in localized (regional) distribution of the oncolytic virus. Expression of the immunostimulatory transgene NAP only in the tumor microenvironment should still be able to effectively elicit an immunostimulatory effect.[38] In contrast, detectable levels of viral RNA were present in most organs following i.v. injection. Most animals had systemic biodistribution at the early time point (day 12) regardless of which dose level they received. In the high-dose group following three i.v. injections, multiple organs (brain, heart, kidney, liver, lung, spinal cord, spleen) harbored viral RNA in modest but appreciable amounts. Even though high levels of RNA were detected in most organs, including the brain, all MV-s-NAP-treated mice appeared healthy throughout the study and exhibited no neurological signs. A previous toxicity study in IFNAR KO-CD46Ge mice that received 1×10^5 or 1×10^7 of the MV-NIS construct (which encodes the sodium iodide symporter) administered i.v. showed MV RNA persistence until day 22 but not on day 91.[46] This is consistent with data from the current study: the i.v.-injected group had detectable MV RNA on day 12 following single injection and on day 54 following multiple injections. In contrast, there was no detectable MV RNA on day 56 following multiple s.c. doses, although virus could be detected on day 11 following a single dose. Taken together, the biodistribution data suggest that intratumoral (s.c.) injection of MV-s-NAP supports viral replication and transgene expression, which is primarily regional at the injection site and persists for a limited period (at least 2 but less than 6 weeks). Despite systemic biodistribution, i.v. administration still resulted in no significant clinical, laboratory, or histologic toxicity.

Antibodies against MV were detected at both time points, administration routes, and MV-s-NAP doses (Figure 6). NAP antibodies were detected at much lower titers and in fewer animals compared with MV. Mice that received single or multiple s.c. treatments exhibited lower titers of MV and NAP antibodies compared with those that received i.v. treatment. These data indicate that locoregional administration of MV-s-NAP, as simulated by s.c. delivery in the current study, generated a limited humoral immune response, whereas i.v. delivery induced a much more substantial antibody response to both the vector and the transgene. The limited systemic humoral immune response following locoregional administration, in combination with the intended targeted delivery within MBC lesions in our trial, support that humoral immunity should not be expected to impact the clinical efficacy of MV-s-NAP in the proposed clinical trial. These data also highlight the safety of this approach: any virus that escapes into the body is expected to be neutralized by a memory response or newly generated anti-MV T and B cells, as even a single dose of virus injected i.v. was sufficient to produce anti-MV titers of 1:12,800–1:20,480, which is substantially higher than the protective titer of >1:120 in humans.[50] In clinical settings where i.v. administration is the desired treatment route, several approaches are available for shielding MV from antibody neutralization, such as polymer coating, measles F and H protein replacement, and an engineered antibody-evading MV construct.[51–54] These methods would require further validation in human trials.

In conclusion, our data demonstrate that both local (s.c.) and systemic (i.v.) administration of MV-s-NAP are well tolerated in non-tumor-bearing IFNAR KO-CD46Ge mice and that no major observable adverse effects arise following treatment at either dose level. These data provided support for a successful IND application that was approved by the FDA. A first-in-human phase I clinical trial using MV-s-NAP to treat patients with MBC (ClinicalTrials.gov: NCT04521764; Figure 7) was initiated in November 2020, and study accrual is ongoing.

MATERIALS AND METHODS

Mice and study design

IFNAR KO-CD46Ge mice were bred in-house; mice were genotyped for IFNAR knockout, and human CD46 expression was confirmed via fluorescent *in situ* hybridization (FISH). Mice were identified by implanted microchips and ear notches. The housing and animal care practices met current Association for Assessment and Accreditation of Laboratory Animal Care International (AAALAC) standards and the current requirements stated in the *Guide for the Care and Use of Laboratory Animals* (National Research Council [NRC], 2011). All animal studies were reviewed and approved in advance by the Mayo Foundation Institutional Animal Care and Use Committee (IACUC).

The study was designed to examine the safety of MV-s-NAP with respect to three parameters: route of administration, dose, and dose frequency (Table 1). Ninety-six 5- to 6-week-old female IFNAR KO-CD46Ge mice were utilized in this study. Only female mice were used due to the intended patient population (women with MBC). The mice were stratified into 6 groups with 2 cohorts (48 mice/cohort). IFNAR KO-CD46Ge mice were treated with 1×10^6 or 1×10^7 $TCID_{50}$ MV-s-NAP or buffer vehicle either s.c., mimicking the direct intratumoral injection planned in the proposed phase I clinical trial, or i.v., to model a worst-case scenario of the virus entering the systemic circulation. Treatment with MV-s-NAP or vehicle was

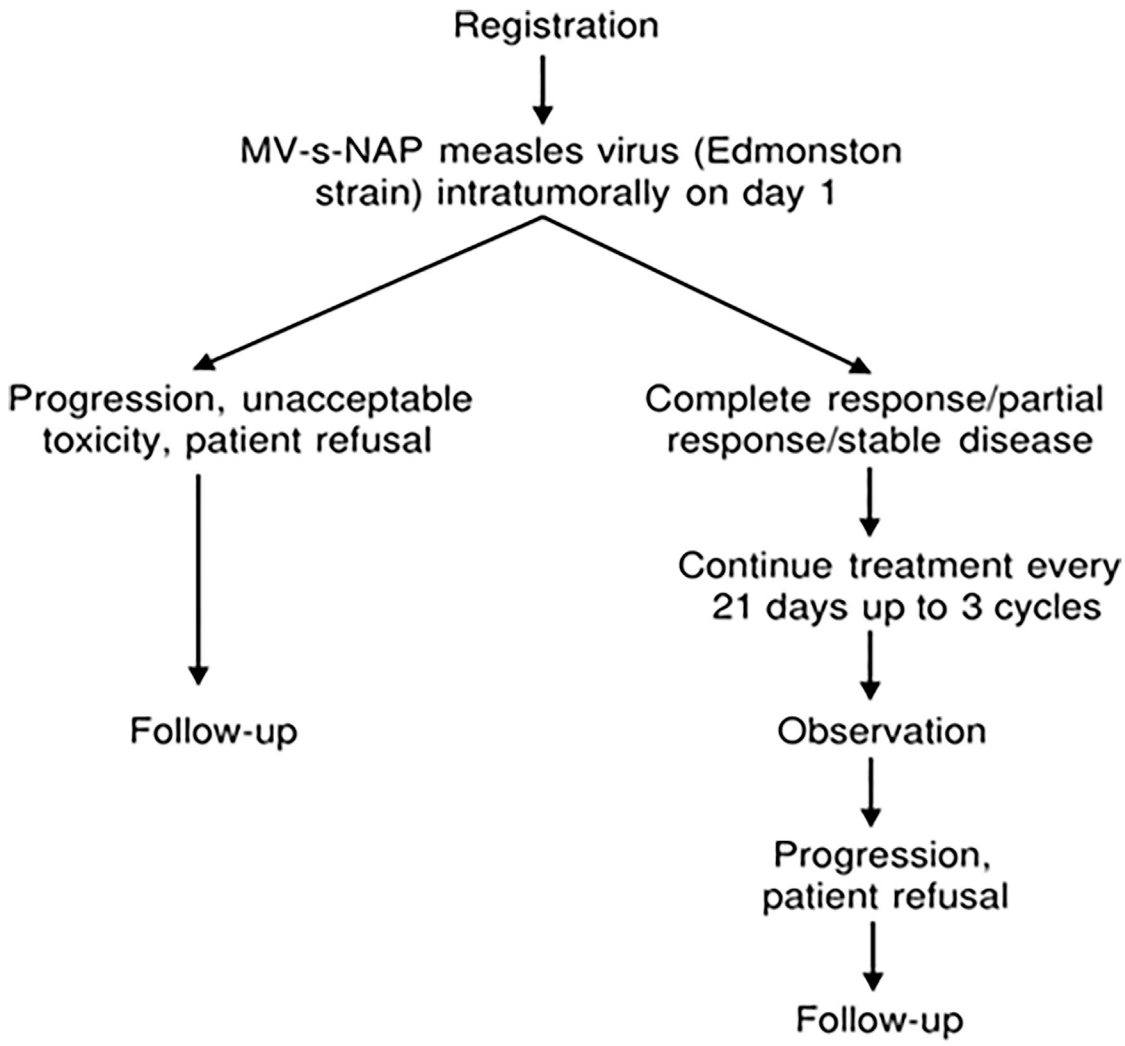

Figure 7. Schema of the phase I clinical trial of intratumoral MV-s-NAP administration to treat metastatic breast cancer (ClinicalTrials.gov: NCT04521764)

started on day 0 using either a single s.c. or i.v. injection or 3 repeated s.c. or i.v. injections given on days 0, 14, and 28. Body weight and clinical signs of ill health were monitored at least 5 times per week. Mice that received a single dose were terminated at day 11 or 12, and the mice that received multiple doses were terminated at day 54 or 56. The dosing scheme was designed to mimic the single- and multiple-dose schema of the human clinical trial (Figure 7).

Virus production and characterization

The test article, MV-s-NAP, was constructed as previously described by the Galanis laboratory.[55] MV-s-NAP was generated by cloning the secretory form of *H. pylori* NAP into the full-length MV plasmid cDNA and rescued on 293-3-46 cells.[55] Clinical-grade vector was produced by the Mayo Clinic Viral Vector Production Laboratory (VVPL, Rochester, MN, USA) and tested for identity, potency, and stability. The titer of the preparation used was 7.9×10^8 $TCID_{50}$/mL, corresponding to 6.9×10^{10} genomes/mL, and was stored at −70°C. Immediately before administration, the virus was thawed and diluted with 0.9% NaCl (Baxter cat. 2B1302, lot: P368894). Virus storage buffer (5% sucrose, 50 mM Tris-HCL [pH 7.4], 2 mM $MgCl_2$; Lonza custom item cat. 08-735, lot: 437,608) was administered to control groups. Test- and control-article mixtures were kept on wet ice throughout the injection procedure.

MV encoding sodium-iodide symporter (MV-NIS) was used as control strain in antigen-mediated enzyme-linked immunosorbent assay (ELISA): its construction has been previously described.[56] Since both MV-NIS and MV-s-NAP are cloned on the same Edmonston B (MV-Edm) vaccine derivative backbone, the expressed MV proteins are identical between the two strains. The only differences between the two strains include the inserted transgene and their position in MV genome: the NIS gene is cloned downstream of the H protein in MV-NIS, while the NAP gene is cloned upstream of N protein in MV-s-NAP.

Treatment schedule

Two days prior to the start of the study, microchips for identification were implanted. Mice were then randomly assigned to treatment groups by body weight. Treatments for all groups began on day 0 as described in Table 1. Briefly, on day 0, groups were randomized into two cohorts based on the route of administration. Necropsy was performed on day 11 or 56 for the s.c. administration groups; on day 12 or 54 for the i.v. administration groups. In each cohort, 8 mice were assigned to one of three treatment groups for injection with virus storage buffer (control), a low MV-s-NAP dose (1×10^6 $TCID_{50}$, corresponding to 8.8×10^7 genomes/dose), or a high MV-s-NAP dose (1×10^7 $TCID_{50}$ corresponding to 8.8×10^8 genomes/dose). Treatment was administered by s.c. or i.v. injection either once (day 0) or every 2 weeks (days 0, 14, and 28).

Clinical observations

Mice were observed for clinical signs (e.g., general appearance, activity) at least five times per week for the duration of the study. Mice were weighed prior to the beginning of the study, weekly during the study, and at necropsy.

Euthanasia and necropsy

Mice were euthanized with inhaled CO_2. Blood was obtained immediately after euthanasia by cardiac puncture. Samples of selected organs tissues were collected, divided, and placed into RNAlater (cat. AM7021, Applied Biosystems, Carlsbad, CA, USA) for quantitative real-time reverse transcription PCR or neutral-buffered 10% formalin (NBF) for histological processing.

Laboratory analysis of peripheral blood

Whole blood was obtained by retro-orbital bleeding of isoflurane-anesthetized mice immediately prior to euthanasia by an experienced lab animal technician, with part of the sample placed in lithium heparin tubes (Becton Dickinson, Franklin Lakes, NJ, USA) for clinical chemistry analysis. Clinical chemistry was analyzed with a Piccolo Xpress Chemistry Analyzer (Abaxis, Union City, CA, USA). Heparinized blood was centrifuged at $8{,}000 \times g$ for 5 min to collect plasma to measure cytokine levels. Retro-orbital blood was also collected in EDTA tubes (Becton Dickinson, Franklin Lakes, NJ, USA) for obtaining a CBC with automated cell differential count. The assay was performed with a VetScan HM5 Hematology Analyzer (Abaxis).

Determination of cytokine levels

Mouse plasma samples, derived from cardiac puncture blood collected at euthanasia, were assayed for mouse GM-CSF, IFN-γ, IL-1β, IL-2, IL-4, IL-5, IL-6, IL-12, IL-13, IL-18, and TNF-α using a ProcartaPlex Mouse Th1/Th2 extended 11-plex kit (EXP110-20820-901; Thermo Fisher Scientific) on a Luminex 200 system (Thermo Fisher Scientific) according to the manufacturer's protocol.

RNA extraction

Total RNA was extracted from selected mouse organs (bone [femur] with bone marrow, brain, heart, intestines [large and small], kidney, liver, lung, lymph node [inguinal], skin [injection site], spinal cord [cervical, thoracic, and lumbar divisions], spleen, and stomach). Tissues were preserved at necropsy in RNAlater (cat. AM7021, Applied Biosystems, Carlsbad, CA, USA) and stored at −20°C. RNA was then harvested as follows: a piece of each tissue was transferred to a new 2-mL sterile Eppendorf tube that contained a 5-mm stainless steel bead. 900-μL Qiazol Lysis Reagent (QIAGEN #1023537, Valencia, CA, USA) was added to each tube. A TissueLyser II instrument was used to disrupt the tissue, and complete homogenization was ensured by operating the TissueLyser II for 2 min at 20 Hz. After each tissue was thoroughly homogenized, sample RNA was extracted using the RNeasy plus Universal Mini kit (QIAGEN #73404) following the manufacturer's protocol. The total RNA concentration of each sample was measured using a NanoQuant Plate on an Infinite M200 instrument (Tecan, Baldwin Park, CA, USA).

Quantitative real-time reverse transcription PCR

Quantitative real-time reverse transcription PCR for nucleocapsid protein RNA (MV-N) was performed on total RNA from the tissue samples collected at necropsy. The assay was optimized for primers, probe, and standard using the TaqManRNA-to-CT 1-Step Kit (Applied Biosystems #4392938, Foster City, CA, USA) and run on a Roche480 machine. The 50-μL quantitative real-time reverse transcription PCR reaction volume was used to amplify an 82-base pair (bp) MV-N genomic RNA target, in the presence of 300-μM each forward and reverse primer, and a 250-μM Blackhole Quencher labeled probe (see below). Each RNA isolate was diluted with RNase-quenching diethylpyrocarbonate (DEPC)-treated water (Invitrogen #AM9906, Waltham, MA, USA) to a concentration of 40 ng/μL. 200 ng or a maximum volume of 5 μL total RNA isolate was used as template in the reaction. One cycle of reverse-transcriptase reaction (15 min at 48°C) is applied, followed by an activation step (10 min at 95°C) and 45 cycles of amplification (15 s at 95°C and 1 min at 60°C), with fluorescence measured during the extension. A standard curve of 10-fold dilutions, containing 1×10^2 to 1×10^7 MV-N gene copies/mL, generated from a purified 82-bp RNA oligonucleotide, was used in the assay. Calculation of copy number was determined using the standard curve and the absolute quantification software of the Roche480 instrument. Primers, probe, and RNA oligonucleotide were ordered from Integrated DNA Technologies (Coralville, IA, USA). Sequences were as follows: forward primer: 5′-GGG TGTGCCGGTTGGA-3′; reverse primer: 5′-AGAAGCCAGGGAG AGCTACAGA-3′; probe: 5'-/56-FAM/TGGGCAGCTCTCGCATC ACTTGC3BHQ_1/-3'; purified 82-bp RNA oligonucleotide used for standard curve: 5′GGGUGUGCCGGUUGGAAGAUGGGCA GCUCUCGCAUCACUUGCUCUGCUGGGCCCGGUUUCUCUG UAGCUCUCCCUGGCUUCU-3'.

Plasma antibody response against MV antigens

96-well ELISA plates (Thermo Fisher Scientific) were coated overnight at 2°C–8°C with 2×10^4 $TCID_{50}$ of heat-inactivated (60°C for 30 min) MV-Edm encoding sodium-iodide symporter (MV-NIS) in 100 μL/well carbonate-bicarbonate buffer (CBB; pH = 9.6). Plates were washed 3 times with phosphate-buffered saline (PBS) and blocked with 1% BSA in PBS. After incubation at room

temperature (RT) for 1 h, the wells were washed with PBS containing 0.05% Tween 20 (PBS/T). Four-fold dilutions of plasma from study mice were made in 1% BSA in PBS/T. 100 μL of the dilutions from 1:200 to 1:819,200 were added to the plate and incubated at RT for 1 h. The last row of wells was incubated only with 1% BSA in PBS/T and was used as the control. Plates were washed 3 times in PBS/T and incubated for 1 h at RT with 1:1,000 horseradish peroxidase (HRP)-conjugated anti-mouse polyvalent immunoglobulins (IgG, IgA, IgM) (#A0412, Sigma) diluted in PBS/T with 1% BSA as the secondary antibody. Plates were washed 5 times in PBS/T and incubated with 100 μL per well of 3, 3′, 5, 5′-tetramethylbenzidine (TMB) substrate (Bethyl Laboratories) for 15 min at RT. The reaction was stopped by adding 50 μL per well of 1M H_3PO_4, after which absorbance (optical density $[OD]_{450}$ nm readings) was measured on an Infinite 200 Pro ELISA plate reader (Tecan). The absorbance of the control wells was subtracted from the sample wells to calculate the endpoint titers.

Plasma antibody response against MV-expressed s-NAP transgene

The recombinant NAP from *H. pylori* strain 26,695 was purified using a Ni-NTA protein purification kit (Qiagen) as previously described.[33] 96-well ELISA plates (Thermo Fisher Scientific) were incubated at 2°C–8°C overnight with 0.3-μg NAP dissolved in 75-μL CBB per well. Plates were washed with PBS and blocked with 1% BSA in PBS at RT for 1h. The plates were washed with PBS/T, and 75-μL 4-fold diluted plasma from study mice (1:20 to 1:81,920 dilutions) was added. Plasma was incubated in parallel plates coated with protein extracts from empty-vector-transfected bacteria as controls.[30] After the incubation for 30 min at RT, ELISA plates were washed three times in PBS/T and incubated for 1 h at RT with 1:1,000 HRP-conjugated anti-mouse polyvalent immunoglobulins (IgG, IgA, IgM) (#A0412, Sigma) diluted (in PBS/T with 1% BSA) as the secondary antibody. Plates were washed 5 times in PBS/T and incubated with 75-μL TMB substrate (Bethyl Laboratories) per well for 15 min at RT. The reaction was stopped using 50 μL per well of 1M H_3PO_4. Absorbance (OD_{450} nm) was read on an Infinite 200 Pro ELISA plate reader (Tecan). The absorbance of the control wells was subtracted from the sample wells to calculate the endpoint titers.

Histological processing and histopathological evaluation of tissue

Selected major organs and tissues (bone [femur] with bone marrow, brain, heart, intestines [large and small], kidney, liver, lung, lymph node [inguinal], skin [injection site], spinal cord [cervical, thoracic, and lumbar divisions], spleen, and stomach) were collected at necropsy at Mayo Clinic Minnesota (Rochester, MN, USA). Tissues were placed in NBF and sent at RT to Mayo Clinic Arizona (Scottsdale, AZ, USA) for routine histological processing into paraffin. Tissue sections were stained with hematoxylin and eosin (H&E) and delivered to an American College of Veterinary Pathologists (ACVP) board-certified veterinary pathologist for evaluation. Findings were scored using a tiered semiquantitative scale with five levels: within normal limits ("normal") or with minimal, mild, moderate, or marked changes. The initial analysis for each animal was done with knowledge of the treatment and dose. Where warranted, a subsequent masked ("blinded") re-evaluation was performed to confirm the existence and severity of findings in some organs (lung and skin) with possible test-article-related effects.

Statistics

Statistical analysis was performed with Prism software v.8.0 (GraphPad Software, San Diego, CA, USA) using both Brown-Forsythe ANOVA and Welch ANOVA tests without assuming equal standard deviations. Statistical significance was set at $p < 0.05$.

DATA AVAILABILITY

All data and supporting materials are available within the article.

ACKNOWLEDGMENTS

The authors would like to thank the Mayo Viral Vector Production Laboratory and the Mayo Toxicology and Pharmacology Shared Resource. This work was funded by National Institutes of Health/National Cancer Institute grants P50CA 116201, P30CA 15083, and R01CA 200507 (E.G.) and a philanthropic grant from Tom and Debby Davidson (E.G. and M.C.L). Graphical abstract illustration was created with BioRender (https://biorender.com) and Photoshop CC 2019.

AUTHOR CONTRIBUTIONS

Conceptualization, E.G., K.W.P., K.B.V., M.B.S., and I.D.I; methodology, E.G., I.D.I., and K.W.P.; formal analysis, M.B.S., B.B., K.B.V., S.C.C. and E.G.; investigation, K.B.V., A.A., M.B.S., N.J., and B.B.; resources, E.G., K.W.P., M.J.F., and M.C.L.; writing – original draft, K.B.V., A.A., S.C.C., B.B., E.P., and I.D.I.; writing – review & editing, all authors; visualization, S.C.C. and K.B.V.; supervision, E.G., K.W.P., and I.D.I.; project administration, E.G., K.W.P., M.C.L., M.P.G., M.J.F., and I.D.I.; funding acquisition, E.G. and M.C.L.

DECLARATION OF INTERESTS

E.G. receives personal compensation as an advisory board member from Kiyatec, Inc., and compensation paid to employer from Karyopharm Therapeutics, Inc. She also receives grant/research/clinical trial funding paid to employer from Servier Pharmaceuticals LLC (formerly Agios Pharmaceuticals, Inc.), Celgene, MedImmune, Inc., and Tracon Pharmaceuticals. K.W.P. and the Mayo Clinic have a financial interest in the technology used in this research. The remaining authors cite no conflicts of interest.

REFERENCES

1. Bray, F., Ferlay, J., Soerjomataram, I., Siegel, R.L., Torre, L.A., and Jemal, A. (2018). Global cancer statistics 2018: GLOBOCAN estimates of incidence and mortality worldwide for 36 cancers in 185 countries. CA Cancer J. Clin. *68*, 394–424. https://doi.org/10.3322/caac.21492.

2. Sledge, G.W., Mamounas, E.P., Hortobagyi, G.N., Burstein, H.J., Goodwin, P.J., and Wolff, A.C. (2014). Past, present, and future challenges in breast cancer treatment. J. Clin. Oncol. *32*, 1979–1986. https://doi.org/10.1200/jco.2014.55.4139.

3. Nielsen, D.L., Andersson, M., and Kamby, C. (2009). HER2-targeted therapy in breast cancer. Monoclonal antibodies and tyrosine kinase inhibitors. Cancer Treat Rev. *35*, 121–136. https://doi.org/10.1016/j.ctrv.2008.09.003.

4. Chia, S., Bedard, P.L., Hilton, J., Amir, E., Gelmon, K., Goodwin, R., Villa, D., Cabanero, M., Tu, D., Tsao, M., and Seymour, L. (2019). A phase ib trial of durvalumab in combination with trastuzumab in HER2-positive metastatic breast cancer (CCTG IND.229). Oncologist *24*, 1439–1445. https://doi.org/10.1634/theoncologist.2019-0321.

5. Mittendorf, E.A., Lu, B., Melisko, M., Price Hiller, J., Bondarenko, I., Brunt, A.M., Sergii, G., Petrakova, K., and Peoples, G.E. (2019). Efficacy and safety analysis of nelipepimut-S vaccine to prevent breast cancer recurrence: a randomized, multicenter, phase III clinical trial. Clin. Cancer Res. *25*, 4248–4254. https://doi.org/10.1158/1078-0432.Ccr-18-2867.

6. Loi, S., Giobbie-Hurder, A., Gombos, A., Bachelot, T., Hui, R., Curigliano, G., Campone, M., Biganzoli, L., Bonnefoi, H., Jerusalem, G., et al. (2019). Pembrolizumab plus trastuzumab in trastuzumab-resistant, advanced, HER2-positive breast cancer (PANACEA): a single-arm, multicentre, phase 1b-2 trial. Lancet Oncol. *20*, 371–382. https://doi.org/10.1016/s1470-2045(18)30812-x.

7. Doniņa, S., Strēle, I., Proboka, G., Auziņš, J., Alberts, P., Jonsson, B., Venskus, D., and Muceniece, A. (2015). Adapted ECHO-7 virus Rigvir immunotherapy (oncolytic virotherapy) prolongs survival in melanoma patients after surgical excision of the tumour in a retrospective study. Melanoma Res. *25*, 421–426. https://doi.org/10.1097/cmr.0000000000000180.

8. Xia, Z.J., Chang, J.H., Zhang, L., Jiang, W.Q., Guan, Z.Z., Liu, J.W., Zhang, Y., Hu, X.H., Wu, G.H., Wang, H.Q., et al. (2004). [Phase III randomized clinical trial of intratumoral injection of E1B gene-deleted adenovirus (H101) combined with cisplatin-based chemotherapy in treating squamous cell cancer of head and neck or esophagus]. Ai Zheng *23*, 1666–1670.

9. Andtbacka, R.H., Kaufman, H.L., Collichio, F., Amatruda, T., Senzer, N., Chesney, J., Delman, K.A., Spitler, L.E., Puzanov, I., Agarwala, S.S., et al. (2015). Talimogene laherparepvec improves durable response rate in patients with advanced melanoma. J. Clin. Oncol. *33*, 2780–2788. https://doi.org/10.1200/jco.2014.58.3377.

10. Ribas, A., Dummer, R., Puzanov, I., VanderWalde, A., Andtbacka, R.H.I., Michielin, O., Olszanski, A.J., Malvehy, J., Cebon, J., Fernandez, E., et al. (2017). Oncolytic virotherapy promotes intratumoral T cell infiltration and improves anti-PD-1 immunotherapy. Cell *170*, 1109–1119.e10. https://doi.org/10.1016/j.cell.2017.08.027.

11. Chesney, J., Puzanov, I., Collichio, F., Singh, P., Milhem, M.M., Glaspy, J., Hamid, O., Ross, M., Friedlander, P., Garbe, C., et al. (2018). Randomized, open-label phase II study evaluating the efficacy and safety of talimogene laherparepvec in combination with ipilimumab versus ipilimumab alone in patients with advanced, unresectable melanoma. J. Clin. Oncol. *36*, 1658–1667. https://doi.org/10.1200/jco.2017.73.7379.

12. Hu, J.C., Coffin, R.S., Davis, C.J., Graham, N.J., Groves, N., Guest, P.J., Harrington, K.J., James, N.D., Love, C.A., McNeish, I., et al. (2006). A phase I study of OncoVEXGM-CSF, a second-generation oncolytic herpes simplex virus expressing granulocyte macrophage colony-stimulating factor. Clin. Cancer Res. *12*, 6737–6747. https://doi.org/10.1158/1078-0432.Ccr-06-0759.

13. Kimata, H., Imai, T., Kikumori, T., Teshigahara, O., Nagasaka, T., Goshima, F., Nishiyama, Y., and Nakao, A. (2006). Pilot study of oncolytic viral therapy using mutant herpes simplex virus (HF10) against recurrent metastatic breast cancer. Ann. Surg Oncol. *13*, 1078–1084. https://doi.org/10.1245/aso.2006.08.035.

14. Bernstein, V., Ellard, S.L., Dent, S.F., Tu, D., Mates, M., Dhesy-Thind, S.K., Panasci, L., Gelmon, K.A., Salim, M., Song, X., et al. (2018). A randomized phase II study of weekly paclitaxel with or without pelareorep in patients with metastatic breast cancer: final analysis of Canadian Cancer Trials Group. Breast Cancer Res. Treat. *167*, 485–493. https://doi.org/10.1007/s10549-017-4538-4.

15. Zeh, H.J., Downs-Canner, S., McCart, J.A., Guo, Z.S., Rao, U.N., Ramalingam, L., Thorne, S.H., Jones, H.L., Kalinski, P., Wieckowski, E., et al. (2015). First-in-man study of western reserve strain oncolytic vaccinia virus: safety, systemic spread, and antitumor activity. Mol. Ther. *23*, 202–214. https://doi.org/10.1038/mt.2014.194.

16. Laurie, S.A., Bell, J.C., Atkins, H.L., Roach, J., Bamat, M.K., O'Neil, J.D., Roberts, M.S., Groene, W.S., and Lorence, R.M. (2006). A phase 1 clinical study of intravenous administration of PV701, an oncolytic virus, using two-step desensitization. Clin. Cancer Res. *12*, 2555–2562. https://doi.org/10.1158/1078-0432.Ccr-05-2038.

17. Noyce, R.S., and Richardson, C.D. (2012). Nectin 4 is the epithelial cell receptor for measles virus. Trends Microbiol. *20*, 429–439. https://doi.org/10.1016/j.tim.2012.05.006.

18. Li, H., Peng, K.W., Dingli, D., Kratzke, R.A., and Russell, S.J. (2010). Oncolytic measles viruses encoding interferon beta and the thyroidal sodium iodide symporter gene for mesothelioma virotherapy. Cancer Gene Ther. *17*, 550–558. https://doi.org/10.1038/cgt.2010.10.

19. Anderson, B.D., Nakamura, T., Russell, S.J., and Peng, K.W. (2004). High CD46 receptor density determines preferential killing of tumor cells by oncolytic measles virus. Cancer Res. *64*, 4919–4926. https://doi.org/10.1158/0008-5472.Can-04-0884.

20. Msaouel, P., Opyrchal, M., Dispenzieri, A., Peng, K.W., Federspiel, M.J., Russell, S.J., and Galanis, E. (2018). Clinical trials with oncolytic measles virus: current status and future prospects. Curr. Cancer Drug Targets *18*, 177–187. https://doi.org/10.2174/1568009617666170222125035.

21. Phuong, L.K., Allen, C., Peng, K.W., Giannini, C., Greiner, S., TenEyck, C.J., Mishra, P.K., Macura, S.I., Russell, S.J., and Galanis, E.C. (2003). Use of a vaccine strain of measles virus genetically engineered to produce carcinoembryonic antigen as a novel therapeutic agent against glioblastoma multiforme. Cancer Res. *63*, 2462–2469.

22. Baldo, A., Galanis, E., Tangy, F., and Herman, P. (2016). Biosafety considerations for attenuated measles virus vectors used in virotherapy and vaccination. Hum. Vaccin. Immunother *12*, 1102–1116. https://doi.org/10.1080/21645515.2015.1122146.

23. Griffin, D.E., and Pan, C.H. (2009). Measles: old vaccines, new vaccines. Curr. Top. Microbiol. Immunol. *330*, 191–212. https://doi.org/10.1007/978-3-540-70617-5_10.

24. Miller, C., Andrews, N., Rush, M., Munro, H., Jin, L., and Miller, E. (2004). The epidemiology of subacute sclerosing panencephalitis in England and Wales 1990-2002. Arch. Dis. Child. *89*, 1145–1148. https://doi.org/10.1136/adc.2003.038489.

25. Maisonneuve, C., Bertholet, S., Philpott, D.J., and De Gregorio, E. (2014). Unleashing the potential of NOD- and Toll-like agonists as vaccine adjuvants. Prod. Natl. Acad. Sci. USA *111*, 12294–12299. https://doi.org/10.1073/pnas.1400478111.

26. Polenghi, A., Bossi, F., Fischetti, F., Durigutto, P., Cabrelle, A., Tamassia, N., Cassatella, M.A., Montecucco, C., Tedesco, F., and de Bernard, M. (2007). The neutrophil-activating protein of Helicobacter pylori crosses endothelia to promote neutrophil adhesion in vivo. J. Immunol. *178*, 1312–1320. https://doi.org/10.4049/jimmunol.178.3.1312.

27. Satin, B., Del Giudice, G., Della Bianca, V., Dusi, S., Laudanna, C., Tonello, F., Kelleher, D., Rappuoli, R., Montecucco, C., and Rossi, F. (2000). The neutrophil-activating protein (HP-NAP) of Helicobacter pylori is a protective antigen and a major virulence factor. J. Exp. Med. *191*, 1467–1476. https://doi.org/10.1084/jem.191.9.1467.

28. Amedei, A., Cappon, A., Codolo, G., Cabrelle, A., Polenghi, A., Benagiano, M., Tasca, E., Azzurri, A., D'Elios, M.M., Del Prete, G., and de Bernard, M. (2006). The neutrophil-activating protein of Helicobacter pylori promotes Th1 immune responses. J. Clin. Invest. *116*, 1092–1101. https://doi.org/10.1172/jci27177.

29. Iankov, I.D., Federspiel, M.J., and Galanis, E. (2013). Measles virus expressed Helicobacter pylori neutrophil-activating protein significantly enhances the immunogenicity of poor immunogens. Vaccine *31*, 4795–4801. https://doi.org/10.1016/j.vaccine.2013.07.085.

30. Iankov, I.D., Penheiter, A.R., Carlson, S.K., and Galanis, E. (2012). Development of monoclonal antibody-based immunoassays for detection of Helicobacter pylori neutrophil-activating protein. J. Immunol. Methods *384*, 1–9. https://doi.org/10.1016/j.jim.2012.06.010.

31. Iankov, I.D., Kurokawa, C.B., D'Assoro, A.B., Ingle, J.N., Domingo-Musibay, E., Allen, C., Crosby, C.M., Nair, A.A., Liu, M.C., Aderca, I., et al. (2015). Inhibition of the Aurora A kinase augments the anti-tumor efficacy of oncolytic measles virotherapy. Cancer Gene Ther. *22*, 438–444. https://doi.org/10.1038/cgt.2015.36.

32. Iankov, I.D., Msaouel, P., Allen, C., Federspiel, M.J., Bulur, P.A., Dietz, A.B., Gastineau, D., Ikeda, Y., Ingle, J.N., Russell, S.J., and Galanis, E. (2010). Demonstration of anti-tumor activity of oncolytic measles virus strains in a malignant pleural effusion breast cancer model. Breast Cancer Res. Treat. *122*, 745–754. https://doi.org/10.1007/s10549-009-0602-z.

33. McDonald, C.J., Erlichman, C., Ingle, J.N., Rosales, G.A., Allen, C., Greiner, S.M., Harvey, M.E., Zollman, P.J., Russell, S.J., and Galanis, E. (2006). A measles virus

vaccine strain derivative as a novel oncolytic agent against breast cancer. Breast Cancer Res. Treat. *99*, 177–184. https://doi.org/10.1007/s10549-006-9200-5.

34. Mrkic, B., Pavlovic, J., Rülicke, T., Volpe, P., Buchholz, C.J., Hourcade, D., Atkinson, J.P., Aguzzi, A., and Cattaneo, R. (1998). Measles virus spread and pathogenesis in genetically modified mice. J. Virol. *72*, 7420–7427. https://doi.org/10.1128/jvi.72.9.7420-7427.1998.

35. McKevitt, T.P., and Lewis, D.J. (2019). Respiratory system. In Toxicologic Pathology: Nonclinical Safety Assessment, Second edition, P.S. Sahota, J.A. Popp, P.R. Bouchard, J.F. Hardisty, and C. Gopinath, eds. (CRC Press (Taylor & Francis)), pp. 515–567.

36. Galanis, E., Atherton, P.J., Maurer, M.J., Knutson, K.L., Dowdy, S.C., Cliby, W.A., Haluska, P., Jr., Long, H.J., Oberg, A., Aderca, I., et al. (2015). Oncolytic measles virus expressing the sodium iodide symporter to treat drug-resistant ovarian cancer. Cancer Res. *75*, 22–30. https://doi.org/10.1158/0008-5472.Can-14-2533.

37. Hardcastle, J., Mills, L., Malo, C.S., Jin, F., Kurokawa, C., Geekiyanage, H., Schroeder, M., Sarkaria, J., Johnson, A.J., and Galanis, E. (2017). Immunovirotherapy with measles virus strains in combination with anti-PD-1 antibody blockade enhances antitumor activity in glioblastoma treatment. Neuro Oncol. *19*, 493–502. https://doi.org/10.1093/neuonc/now179.

38. Panagioti, E., Kurokawa, C., Viker, K., Ammayappan, A., Anderson, S.K., Sotiriou, S., Chatzopoulos, K., Ayasoufi, K., Johnson, A.J., Iankov, I.D., and Galanis, E. (2021). Immunostimulatory bacterial antigen-armed oncolytic measles virotherapy significantly increases the potency of anti-PD1 checkpoint therapy. J. Clin. Invest. *131*. https://doi.org/10.1172/jci141614.

39. Allen, C., Paraskevakou, G., Liu, C., Iankov, I.D., Msaouel, P., Zollman, P., Myers, R., Peng, K.W., Russell, S.J., and Galanis, E. (2008). Oncolytic measles virus strains in the treatment of gliomas. Expert. Opin. Biol. Ther. *8*, 213–220. https://doi.org/10.1517/14712598.8.2.213.

40. Peng, K.W., Frenzke, M., Myers, R., Soeffker, D., Harvey, M., Greiner, S., Galanis, E., Cattaneo, R., Federspiel, M.J., and Russell, S.J. (2003). Biodistribution of oncolytic measles virus after intraperitoneal administration into Ifnar-CD46Ge transgenic mice. Hum. Gene Ther. *14*, 1565–1577. https://doi.org/10.1089/104303403322495070.

41. Alemany, R., Suzuki, K., and Curiel, D.T. (2000). Blood clearance rates of adenovirus type 5 in mice. J. Gen. Virol. *81*, 2605–2609. https://doi.org/10.1099/0022-1317-81-11-2605.

42. Varnavski, A.N., Calcedo, R., Bove, M., Gao, G., and Wilson, J.M. (2005). Evaluation of toxicity from high-dose systemic administration of recombinant adenovirus vector in vector-naive and pre-immunized mice. Gene Ther. *12*, 427–436. https://doi.org/10.1038/sj.gt.3302347.

43. Zhang, L., Steele, M.B., Jenks, N., Grell, J., Suksanpaisan, L., Naik, S., Federspiel, M.J., Lacy, M.Q., Russell, S.J., and Peng, K.W. (2016). Safety studies in tumor and non-tumor-bearing mice in support of clinical trials using oncolytic VSV-IFNβ-NIS. Hum. Gene. Ther. Clin. Dev. *27*, 111–122. https://doi.org/10.1089/humc.2016.061.

44. Lal, S., Peng, K.W., Steele, M.B., Jenks, N., Ma, H., Kohanbash, G., Phillips, J.J., and Raffel, C. (2016). Safety study: intraventricular injection of a modified oncolytic measles virus into measles-immune, hCD46-transgenic, IFNαRko mice. Hum. Gene Ther. Clin. Dev. *27*, 145–151. https://doi.org/10.1089/humc.2016.062.

45. Mrkic, B., Odermatt, B., Klein, M.A., Billeter, M.A., Pavlovic, J., and Cattaneo, R. (2000). Lymphatic dissemination and comparative pathology of recombinant measles viruses in genetically modified mice. J. Virol. *74*, 1364–1372. https://doi.org/10.1128/jvi.74.3.1364-1372.2000.

46. Myers, R.M., Greiner, S.M., Harvey, M.E., Griesmann, G., Kuffel, M.J., Buhrow, S.A., Reid, J.M., Federspiel, M., Ames, M.M., Dingli, D., et al. (2007). Preclinical pharmacology and toxicology of intravenous MV-NIS, an oncolytic measles virus administered with or without cyclophosphamide. Clin. Pharmacol. Ther. *82*, 700–710. https://doi.org/10.1038/sj.clpt.6100409.

47. Völker, I., Bach, P., Coulibaly, C., Plesker, R., Abel, T., Seifried, J., Heidmeier, S., Mühlebach, M.D., Lauer, U.M., and Buchholz, C.J. (2013). Intrahepatic application of suicide gene-armed measles virotherapeutics: a safety study in transgenic mice and rhesus macaques. Hum. Gene Ther. Clin. Dev. *24*, 11–22. https://doi.org/10.1089/humc.2012.242.

48. de Vries, R.D., Lemon, K., Ludlow, M., McQuaid, S., Yüksel, S., van Amerongen, G., Rennick, L.J., Rima, B.K., Osterhaus, A.D., de Swart, R.L., and Duprex, W.P. (2010). In vivo tropism of attenuated and pathogenic measles virus expressing green fluorescent protein in macaques. J. Virol. *84*, 4714–4724. https://doi.org/10.1128/jvi.02633-09.

49. Myers, R., Harvey, M., Kaufmann, T.J., Greiner, S.M., Krempski, J.W., Raffel, C., Shelton, S.E., Soeffker, D., Zollman, P., Federspiel, M.J., et al. (2008). Toxicology study of repeat intracerebral administration of a measles virus derivative producing carcinoembryonic antigen in rhesus macaques in support of a phase I/II clinical trial for patients with recurrent gliomas. Hum. Gene Ther. *19*, 690–698. https://doi.org/10.1089/hum.2008.035.

50. Chen, R.T., Markowitz, L.E., Albrecht, P., Stewart, J.A., Mofenson, L.M., Preblud, S.R., and Orenstein, W.A. (1990). Measles antibody: reevaluation of protective titers. J. Infect. Dis. *162*, 1036–1042. https://doi.org/10.1093/infdis/162.5.1036.

51. Bah, E.S., Nace, R.A., Peng, K.W., Muñoz-Alía, M., and Russell, S.J. (2020). Retargeted and stealth-modified oncolytic measles viruses for systemic cancer therapy in measles immune patients. Mol. Cancer Ther. *19*, 2057–2067. https://doi.org/10.1158/1535-7163.Mct-20-0134.

52. Hudacek, A.W., Navaratnarajah, C.K., and Cattaneo, R. (2013). Development of measles virus-based shielded oncolytic vectors: suitability of other paramyxovirus glycoproteins. Cancer Gene Ther. *20*, 109–116. https://doi.org/10.1038/cgt.2012.92.

53. Muñoz-Alía, M., Nace, R.A., Zhang, L., and Russell, S.J. (2021). Serotypic evolution of measles virus is constrained by multiple co-dominant B cell epitopes on its surface glycoproteins. Cell Rep. Med. *2*, 100225. https://doi.org/10.1016/j.xcrm.2021.100225.

54. Nosaki, K., Hamada, K., Takashima, Y., Sagara, M., Matsumura, Y., Miyamoto, S., Hijikata, Y., Okazaki, T., Nakanishi, Y., and Tani, K. (2016). A novel, polymer-coated oncolytic measles virus overcomes immune suppression and induces robust antitumor activity. Mol. Ther. Oncol. *3*, 16022. https://doi.org/10.1038/mto.2016.22.

55. Iankov, I.D., Haralambieva, I.H., and Galanis, E. (2011). Immunogenicity of attenuated measles virus engineered to express Helicobacter pylori neutrophil-activating protein. Vaccine *29*, 1710–1720. https://doi.org/10.1016/j.vaccine.2010.12.020.

56. Dingli, D., Peng, K.W., Harvey, M.E., Greipp, P.R., O'Connor, M.K., Cattaneo, R., Morris, J.C., and Russell, S.J. (2004). Image-guided radiovirotherapy for multiple myeloma using a recombinant measles virus expressing the thyroidal sodium iodide symporter. Blood *103*, 1641–1646. https://doi.org/10.1182/blood-2003-07-2233.